

Supporting Information

Dinuclear copper(II) complexes containing oxamate and blocking ligands: crystal structure, magnetic properties and DFT calculations

Tatiana R. G. Simões,^a Wallace D. do Pim,^b Karina C. Metz,^a Marcos A. Ribeiro,^c
Daniel C. A. Valente,^d Thiago M. Cardozo,^d Carlos B. Pinheiro,^e Emerson F. Pedroso,^b
Bruno A. C. Horta,^d Cynthia L. M. Pereira,^f Gilmar P. de Souza,^g Humberto O.
Stumpf^{f*}

^a*Departamento de Química, Universidade Federal do Paraná, Centro Politécnico, Curitiba, PR, 81530-900, Brazil.*

^b*Departamento de Química, Centro Federal de Educação Tecnológica de Minas Gerais, Av. Amazonas, 5253, Belo Horizonte, MG, 30421-169, Brazil.*

^c*Departamento de Química, Universidade Federal do Espírito Santo, Av. Fernando Ferrari, 514, Goiabeiras, Vitória, ES, 29075-910, Brazil.*

^d*Instituto de Química, Universidade Federal do Rio de Janeiro, 21941-909, Rio de Janeiro/RJ, Brazil.*

^e*Departamento de Física, ICEX, Universidade Federal de Minas Gerais, Av. Antônio Carlos 6627, Belo Horizonte, MG, 31270-901, Brazil.*

^f*Departamento de Química, ICEX, Universidade Federal de Minas Gerais, Av. Antônio Carlos 6627, Belo Horizonte, MG, 31270-901, Brazil.*

^g*Departamento de Química, ICEB, Universidade Federal de Ouro Preto, Campus Universitário Morro do Cruzeiro, Ouro Preto-MG, 35400-000, Brazil.*

Corresponding author: tatiana.renata@ufpr.br and stumpf@ufmg.br

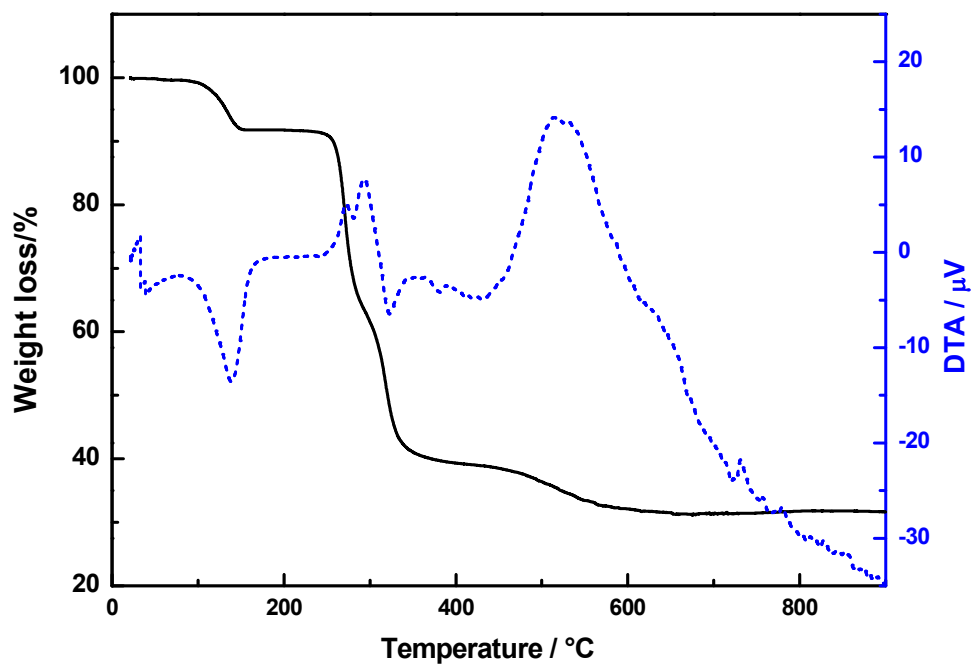


Figure S1: TG of 1

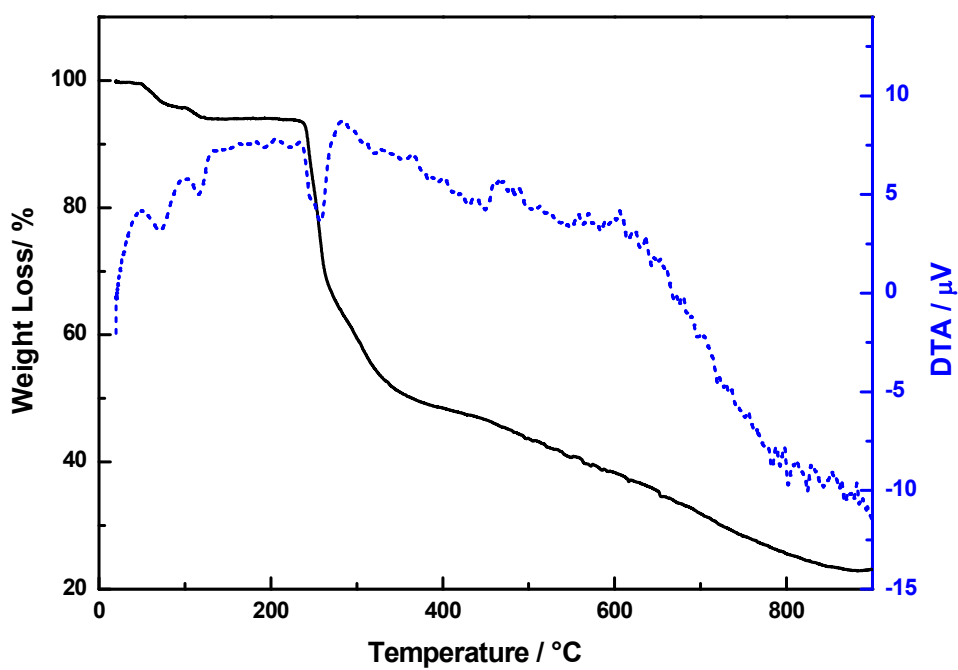


Figure S2: TG of 2

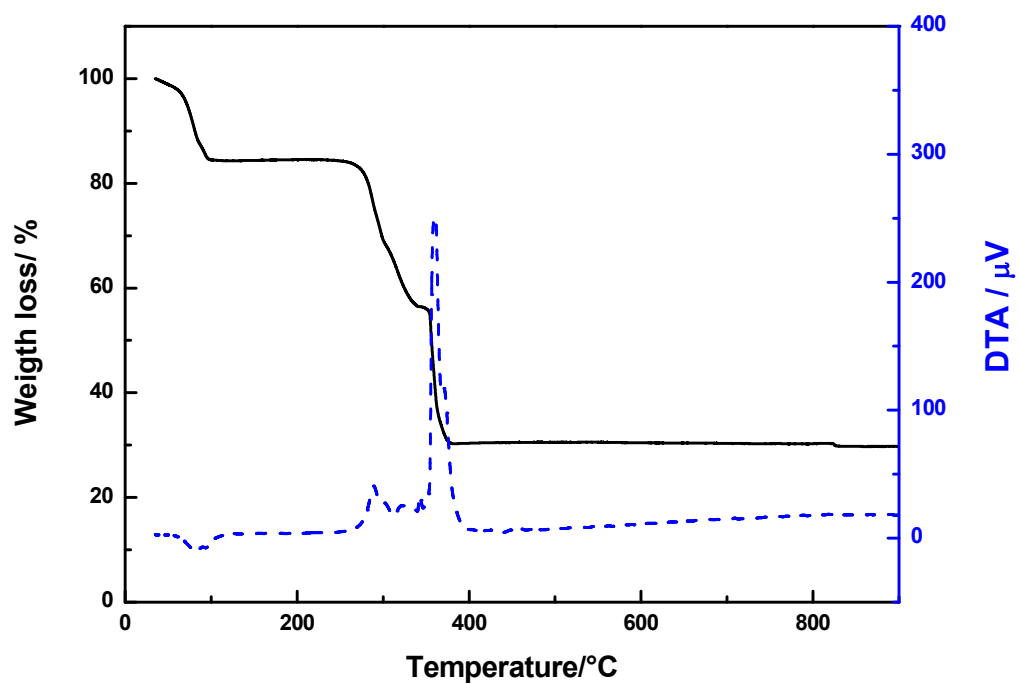


Figure S3: TG of 3

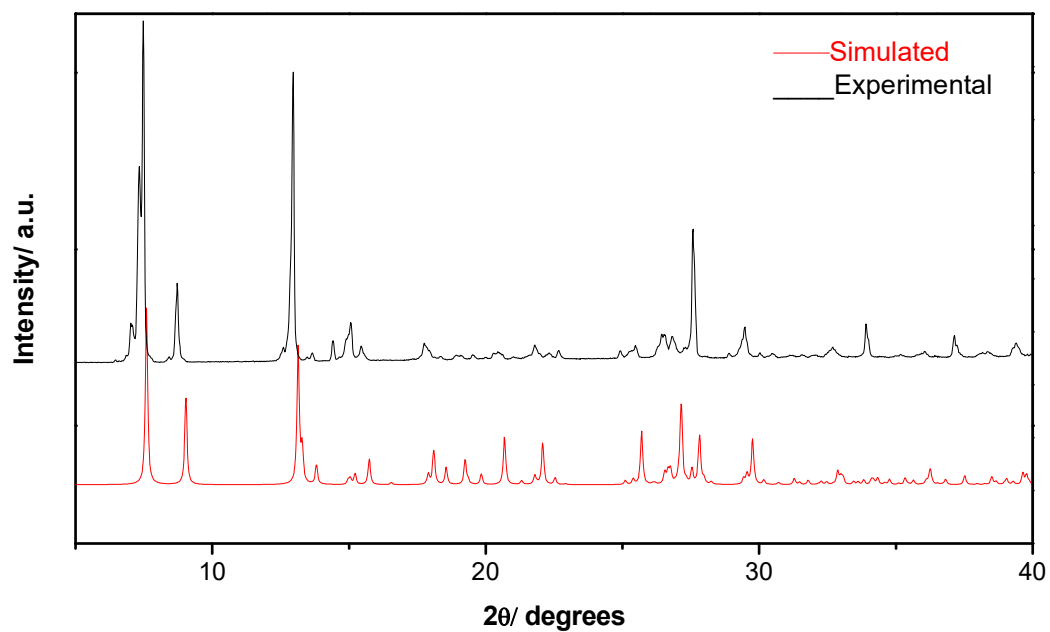


Figure S4: Experimental (black) and calculated (red) XRD patterns of 1.

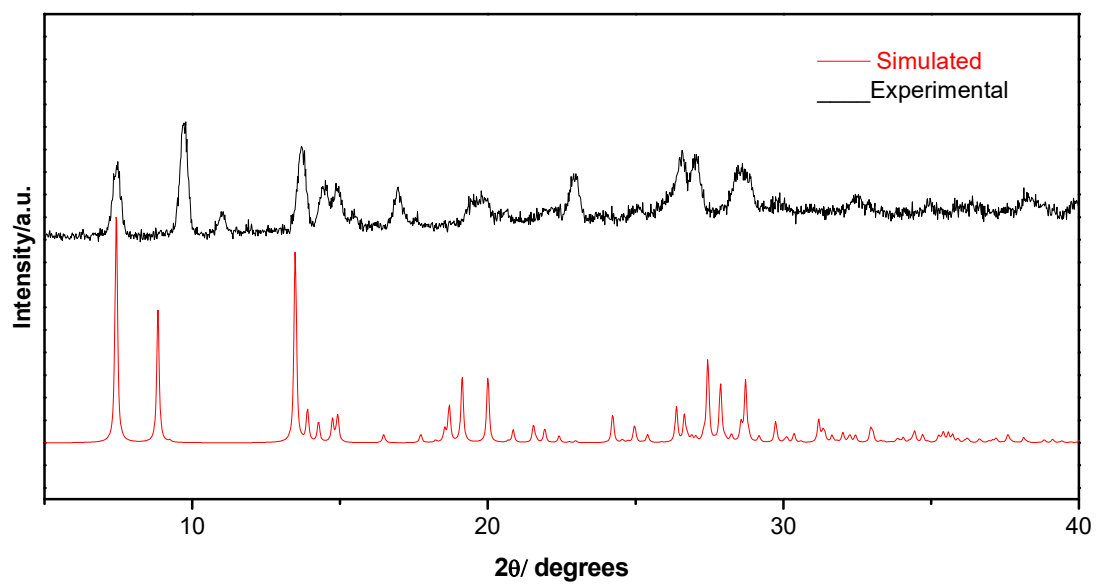


Figure S5: Experimental (black) and calculated (red) XRD patterns of **2**.

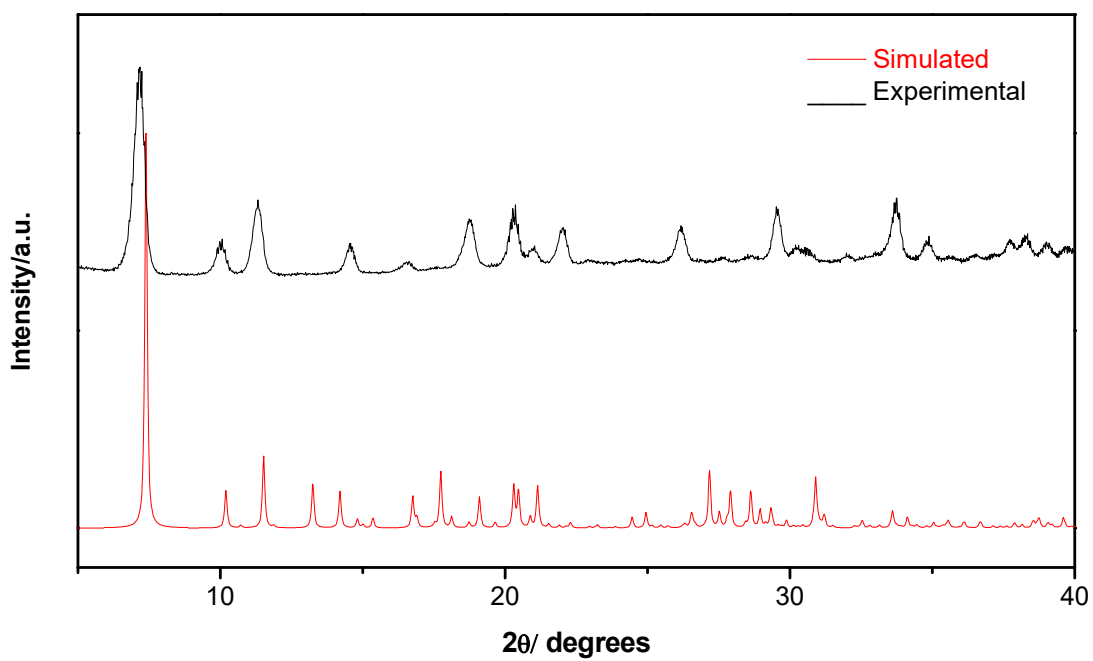


Figure S6: Experimental (black) and calculated (red) XRD patterns of **3**.

Table S1. Hydrogen-bond geometry (Å, °) for Compound **1**

$D-H\cdots A$	$D-H$	$H\cdots A$	$D\cdots A$	$D-H\cdots A$
$C6-H6\cdots OW2^i$	0.93	2.74	3.404 (4)	130
$C8-H8\cdots OW1^{ii}$	0.93	2.64	3.344 (4)	133
$N4-H4A\cdots O5^{iii}$	0.97	2.21	3.099 (4)	152
$N4-H4B\cdots O6^{iv}$	0.97	2.21	2.907 (4)	128
$N4-H4B\cdots O5^{iv}$	0.97	2.52	3.416 (4)	153
$N3-H3B\cdots O1^v$	0.97	2.20	3.051 (4)	145
$OW2-HW2A\cdots O2^{iii}$	0.82	2.19	3.007 (4)	178
$OW2-HW2A\cdots O5^{iii}$	0.82	2.61	3.165 (4)	127
$OW2-HW2B\cdots O5^{vi}$	0.83	2.06	2.873 (4)	167
$OW1-HW1A\cdots O6^{vi}$	0.85	1.88	2.724 (3)	175
$OW1-HW1B\cdots OW2$	0.85	1.90	2.734 (4)	166

Symmetry codes: (i) $-x, -y, -z+3$; (ii) $x+1, y-1, z$; (iii) $x, y, z+1$; (iv) $-x+1, -y, -z+2$; (v) $-x, -y+1, -z+2$; (vi) $-x, -y, -z+2$.

Table S2. Hydrogen-bond geometry (Å, °) for Compound **2**

$D-H\cdots A$	$D-H$	$H\cdots A$	$D\cdots A$	$D-H\cdots A$
$N4-H4B\cdots OW2$	0.91	2.06	2.935 (4)	160
$OW3-HW3A\cdots O7^i$	0.82 (6)	2.01 (6)	2.757 (4)	153 (5)
$OW3-HW3B\cdots O2$	0.81 (6)	2.08 (6)	2.876 (3)	167 (5)
$OW1-HW1B\cdots O6^{ii}$	0.86 (2)	1.92 (2)	2.774 (3)	173 (4)
$OW2-HW2\cdots O5^{ii}$	0.85 (2)	1.94 (2)	2.771 (4)	168 (5)
$O7-H7A\cdots OW3^{iii}$	0.84 (2)	1.94 (2)	2.760 (4)	164 (5)

Symmetry codes: (i) $-x+3/2, -y+1/2, -z+1$; (ii) $-x+1, -y+1, -z+1$; (iii) $x, -y, z-1/2$.

Table S3. Hydrogen-bond geometry (Å, °) for Compound **3**

$D-H\cdots A$	$D-H$	$H\cdots A$	$D\cdots A$	$D-H\cdots A$
O3 <i>W</i> — H3 <i>WA</i> ⋯O5	0.87	1.88	2.7420 (17)	173
O3 <i>W</i> — H3 <i>WB</i> ⋯O3 ⁱ	0.87	1.96	2.8049 (16)	164
O5 <i>W</i> — H5 <i>WA</i> ⋯O4 <i>W</i>	0.87	1.88	2.721 (2)	163
O5 <i>W</i> — H5 <i>WB</i> ⋯O5	0.87	2.18	2.9439 (17)	146
O2 <i>W</i> — H2 <i>WB</i> ⋯O3 <i>W</i> ⁱⁱ	0.87	1.93	2.7918 (19)	173
O1 <i>W</i> — H1 <i>WB</i> ⋯O2 <i>W</i>	0.85	1.88	2.7243 (18)	178
O4 <i>W</i> — H4 <i>WA</i> ⋯O3 <i>W</i> ⁱⁱⁱ	0.85 (1)	2.01 (1)	2.7953 (18)	153 (2)
O4 <i>W</i> — H4 <i>WB</i> ⋯O5 <i>W</i> ^{iv}	0.85 (1)	1.97 (1)	2.7549 (19)	154 (2)

Symmetry codes: (i) $x, -y+1/2, z-1/2$; (ii) $x+1, -y+1/2, z+1/2$; (iii) $x+1, y, z$; (iv) $-x+1, -y, -z+1$.

Theoretical Calculations

Several articles have already emphasized the fluctuation of exchange coupling constants predicted by broken symmetry DFT calculations¹⁻³. Accordingly, a group of representative functionals was tested for compound **1**, and their results are presented in Table S4. In these preliminary calculations, a smaller basis set was used, composed of zora-def2-TZVP for copper atoms and its SVP analogue for all the others. The RIJCOSX approximation was used as well as the recommended sarc/J (decontracted def2/J) auxiliary basis set for all atoms. Based on these results the BHandHLYP was chosen for further calculations.

Previous articles have analyzed the basis set effect^{3,4} and a small test was also performed in the present study. Two subsequent tests were performed to check the effect of basis set size and integration grid size. Based on Tables S5 and S6, the default grid size and increasing the basis set only on the copper centers are sufficient for converged results. In this particular case, the basis zora-def2-TZVP on copper atoms appears to provide better results than zora-def2-QZVPP (Table S6), but this can only be

due to spurious cancellations of errors, which might not occur in the other compounds. Hence, as the basis set with zora-def2-QZVPP only on copper atoms provides results close to the largest basis tested (around 13 cm⁻¹ error) within reasonable calculation wall-time, it was the one chosen to produce results included in the main text. Similar basis sets have also been used in previously reported studies^{1,4}. Lastly, the RIJCOSX has no significant impact on the calculated coupling value, as its effects are smaller than the one caused by basis set.

Bond orders were estimated following Löwdin^{5,6} and Mayer schemes^{7,8} and results are presented in Table S7. Cu2-O3 and Cu2-O4 (Figures 5 and 6) are bonds between a copper center and two equatorial oxygens, and Cu2-O1W is the bond between the same copper and an axially coordinated water. Both bond orders schemes estimate that the bond between a copper center and the oxygen of the other monomer (Cu2-O6) is even weaker than the copper-water coordination.

Lastly, to further test the model used to analyze experimental results, coupling strengths between all pairs of copper atoms were calculated for compound **3** as a dinuclear and also considering the complex as a tetranuclear system of four copper(II) units, as shown in Figures 6, S11 and S12, using the substitution by diamagnetic Zn(II)⁹, and results are shown in Table S9. All couplings between centers of different monomers are negligible, providing further support for the model used (all compounds as dinuclear) and an explanation for its validity: the overlap between these centers is much smaller than between those in the same monomer. The agreement with experiment for the $J(\text{Cu1}, \text{Cu2})$ coupling is also better if compound **3** is treated as dinuclear instead of as tetranuclear (compare Tables 4 and S9), although the error in the latter, around 25%, is still close to the expected for a broken-symmetry calculation¹⁰. This difference in results might be associated to any of the chosen functional's specific deficiencies such as a lack of dispersion corrections since this contribution should be more important in the dimer calculation than in the monomer. However, both theoretical and experimental results are consistent with each other, and the inclusion of dispersion is not expected to provide further insights (only perhaps better agreement between results in Tables 4 and Table S9). In summary, the theoretical results presented in Tables 4 and S9, as well as the bond order estimates (Table S7) for the bonding strength between Cu2 and O6 (Figure 6) in compound **3**, predicted to be quite weak, indicate that all three compounds magnetic couplings are of an intramolecular nature.

Table S4. Preliminary calculated exchange coupling constants for compound **1**, in order to choose functional. All calculations used ZORA, RIJCOSX with sarc/j auxiliary basis, zora-def2-tzvp for copper and zora-def2-svp for other atoms basis sets. Also shown are the corresponding orbitals overlap ($S_{\alpha\beta}$) and the Hartree-Fock exchange. RS stands for range-separated.

Mapping used for J (cm^{-1})	Compound 1, functional test with smaller basis						
	PBE0 ¹¹	B3LYP ^{12,13}	M06 ¹⁴	M06-2X ¹⁴	CAM-B3LYP ¹⁵	BHandHLYP ¹⁶	wb97-XD ¹⁷
J^{Noo}	-1302.8	-2312.0	-2428.4	-216.3	-645.3	-203.1	-551.7
J^{Ruiz}	-651.4	-1156.0	-1214.2	-108.1	-322.6	-101.6	-275.8
J^{Yam}	-1195.4	-1925.3	-1991.4	-215.6	-631.0	-202.5	-543.4
J^{Exp}	-183.5						
$S_{\alpha\beta}$	0.30	0.45	0.47	0.06	0.15	0.06	0.13
Hartree-Fock exchange (%)	25	20	27	54	RS	50	RS

Table S5. Preliminary calculated exchange coupling constants for compound **1**, to test grid's effect. All calculations used BHandHLYP and ZORA. Using ORCA's keywords, "Smaller" is the default grid, and "Larger" is "Grid6 nofinalgrid". J^{Yam} was omitted as it didn't add new information.

Compound 1, grid and RIJCOSX test with BHandHLYP				
DFT integration grid	RIJCOSX	Basis set	J^{Noo}	J^{Ruiz}
Smaller	on	zora-def2-TZVP Cu / zora-def2-SVP other atoms	-203.12	-101.56
Larger			-203.10	-101.55
Smaller	off		-203.41	-101.71
Larger			-203.40	-101.70
Smaller	on	zora-def2-QZVPP on all atoms	-199.59	-99.80
Smaller	off		-200.11	-100.06
Larger			-199.88	-99.94

Table S6. Preliminary calculated exchange coupling constants for compound **1**, to test basis set effect. All calculations used BHandHLYP functional, ZORA and RIJCOSX with sarc/j auxiliary basis.

Compound 1, basis set test with functional BhandHLYP					
Basis set on copper atoms	Basis set on other atoms	J (cm ⁻¹)			Basis set dimension
		J^{Noo}	J^{Ruiz}	J^{Yam}	
	zora-def2-QZVPP	-199.6	-99.8	-199.0	2220
zora-def2-QZVPP	zora-def2-TZVP	-200.9	-100.4	-200.3	1138
	zora-def2-SVP	-186.7	-93.3	-186.2	670
zora-def2-TZVP	zora-def2-SVP	-203.1	-101.6	-202.5	550

Table S7. Calculated bond orders for compound **3** tetranuclear dimer (Figures 5 and 6). Values for analogous atom pairs in the other compounds are also shown. All calculations used BHandHLYP functional, with zora-def2-QZVPP for copper/zora-def2-SVP for other atoms, ZORA and RIJCOSX with sarc/j auxiliary basis.

Compound	Bond order scheme	Equatorial ligands		Axial ligands	
		Cu2-O3	Cu2-O4	Cu2-O1W	Cu2-O6
1	Löwdin	1.1	1.12	0.72	0.28
	Mayer	0.62	0.69	0.35	0.24
2	Löwdin	1.1	1.11	0.71	0.35
	Mayer	0.67	0.61	0.38	0.29
3	Löwdin	1.13	1.12	0.68	0.38
	Mayer	0.68	0.62	0.38	0.3

Table S8. Calculated Mulliken spin densities for selected atoms, for high-spin (HS) and broken symmetry (BS) states. For numbering scheme, see Figures 1, 3 and 5. All calculations used BHandHLYP functional, with zora-def2-QZVPP for copper/zora-def2-SVP for other atoms, ZORA and RIJCOSX with sarc/j auxiliary basis.

Mulliken spin density for selected atoms						
Atom label	Compound 1		Compound 2		Compound 3	
	HS	BS	HS	BS	HS	BS
Cu1	0.72	0.72	0.73	0.73	0.72	0.72
Cu2	0.78	-0.78	0.78	-0.77	0.77	-0.77
O1	0.03	0.02	0.03	0.02	0.03	0.03
O2	0.06	0.06	0.06	0.06	0.06	0.06
O3	0.05	-0.05	0.05	-0.05	0.05	-0.05
O4	0.05	-0.05	0.05	-0.06	0.05	-0.06
N1	0.08	0.08	0.08	0.08	0.08	0.08
N2	0.12	0.11	0.11	0.11	0.12	0.11
N3	0.06	-0.05	0.06	-0.06	0.06	-0.06
N4	0.06	-0.06	0.06	-0.06	0.06	-0.06

Table S9. Calculated exchange coupling constants and corresponding orbitals overlap ($S_{\alpha\beta}$) for compound **3** treated as a tetranuclear dimer (Figures 6). For each pair of copper atoms, the exchange coupling was calculated substituting the other pair by diamagnetic Zn(II). J^{Ruiz} and J^{Yam} were omitted. High-spin and broken symmetry states are shown in Figures S11 and S12. The functional BHandHLYP was used, with zora-def2-QZVPP basis set on copper and zinc, and zora-def2-SVP on all other atoms.

Procedure to obtain J (cm^{-1})	Compound 3 as tetranuclear complex			
	$J(\text{Cu1,Cu2})$	$J(\text{Cu1,Cu1}^i)$	$J(\text{Cu2,Cu2}^i)$	$J(\text{Cu1,Cu2}^i)$
J^{Noo}	-147.8	Absolute value < 1		
J^{Exp}	-195.6	Negligible		
$S_{\alpha\beta}$	0.04	< 0.001		

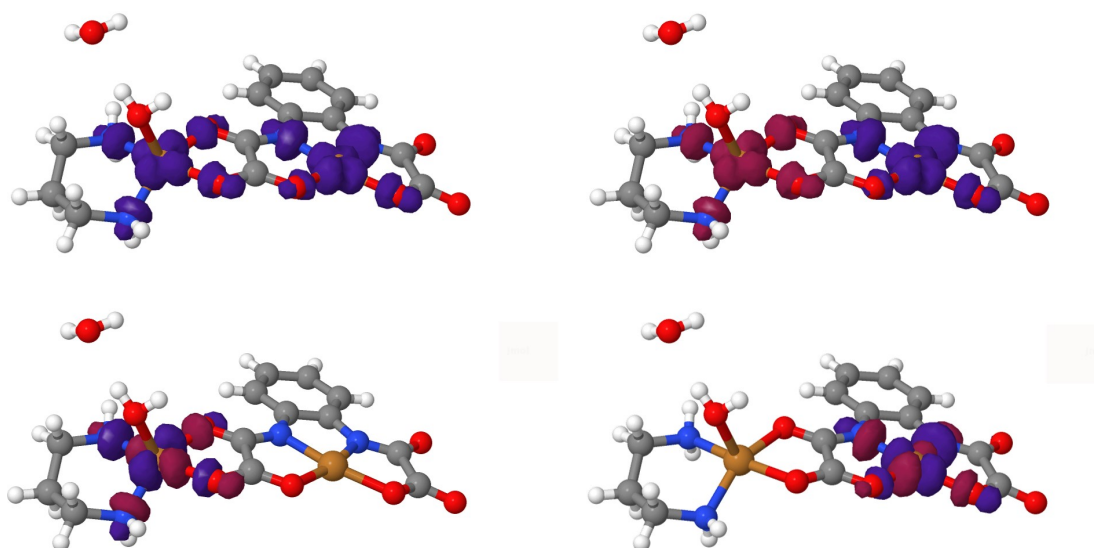


Figure S7: Spin density for the triplet (high-spin, upper left) and broken symmetry (upper right) states, with contour value 0.003 a.u., and corresponding orbitals (bottom), with contour value 0.04 a.u., for compound **1**. Positive values are blue, and negative, red. Color code: Cu (yellow), N (blue), O (red), H (white), C (gray).

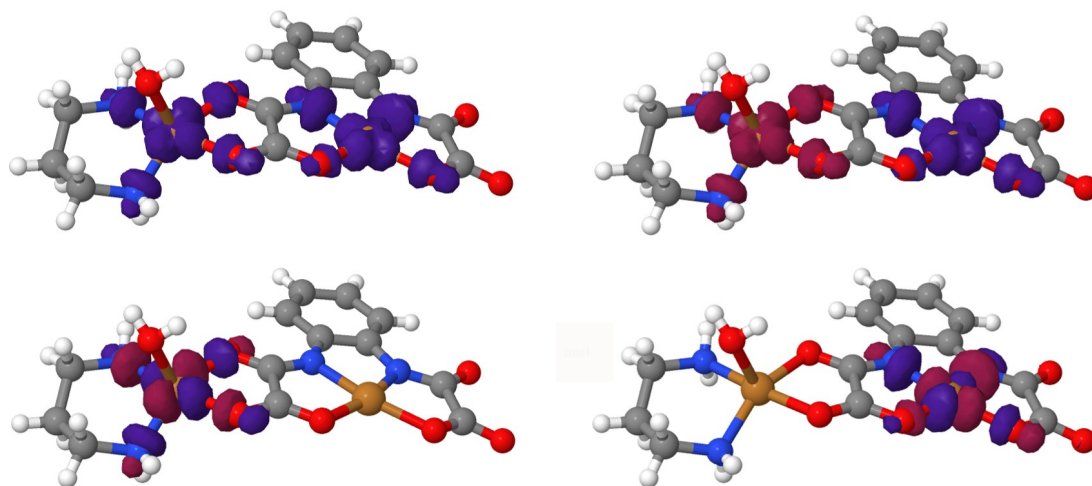


Figure S8: Spin density for the triplet (high-spin, upper left) and broken symmetry (upper right) states, with contour value 0.003 a.u., and corresponding orbitals (bottom), with contour value 0.04 a.u, for compound **1**, removing one molecule of water (compare with Figure S7). Positive values are blue, and negative, red. Color code: Cu (yellow), N (blue), O (red), H (white), C (gray).

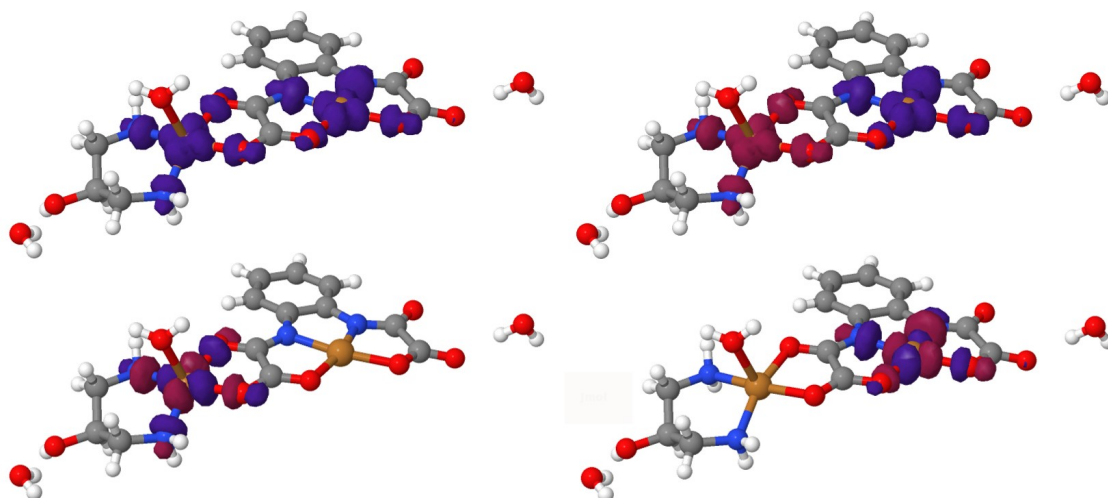


Figure S9: Spin density for the triplet (high-spin, upper left) and broken symmetry (upper right) states, with contour value 0.003 a.u., and corresponding orbitals (bottom), with contour value 0.04 a.u, for compound **2**. Positive values are blue, and negative, red. Some water molecules (right and left) were excluded for easier visualization. Color code: Cu (yellow), N (blue), O (red), H (white), C (gray).

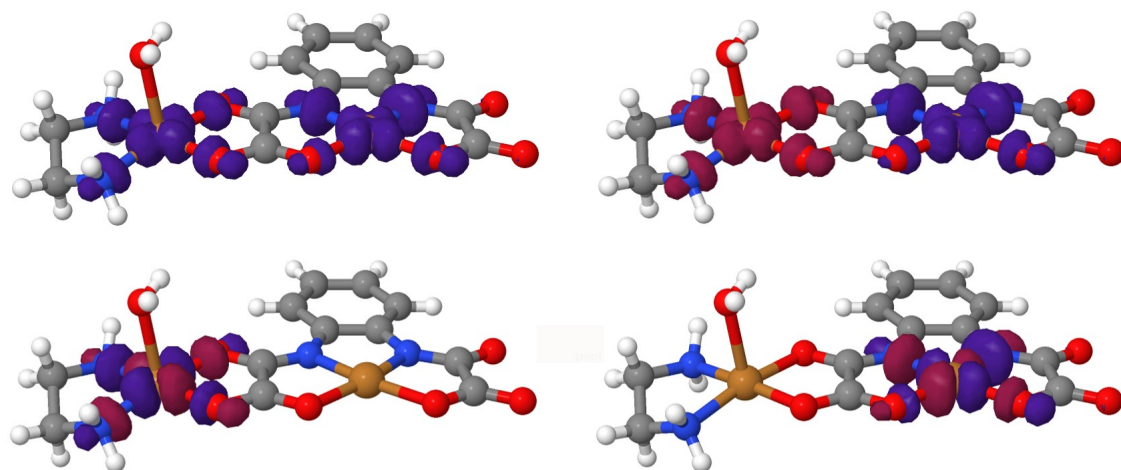


Figure S10: Spin density for the triplet (high-spin, upper left) and broken symmetry (upper right) states, with contour value 0.003 a.u., and corresponding orbitals (bottom), with contour value 0.04 a.u., for compound **3**, when calculated as a dinuclear monomer. Positive values are blue, and negative, red. Color code: Cu (yellow), N (blue), O (red), H (white), C (gray).

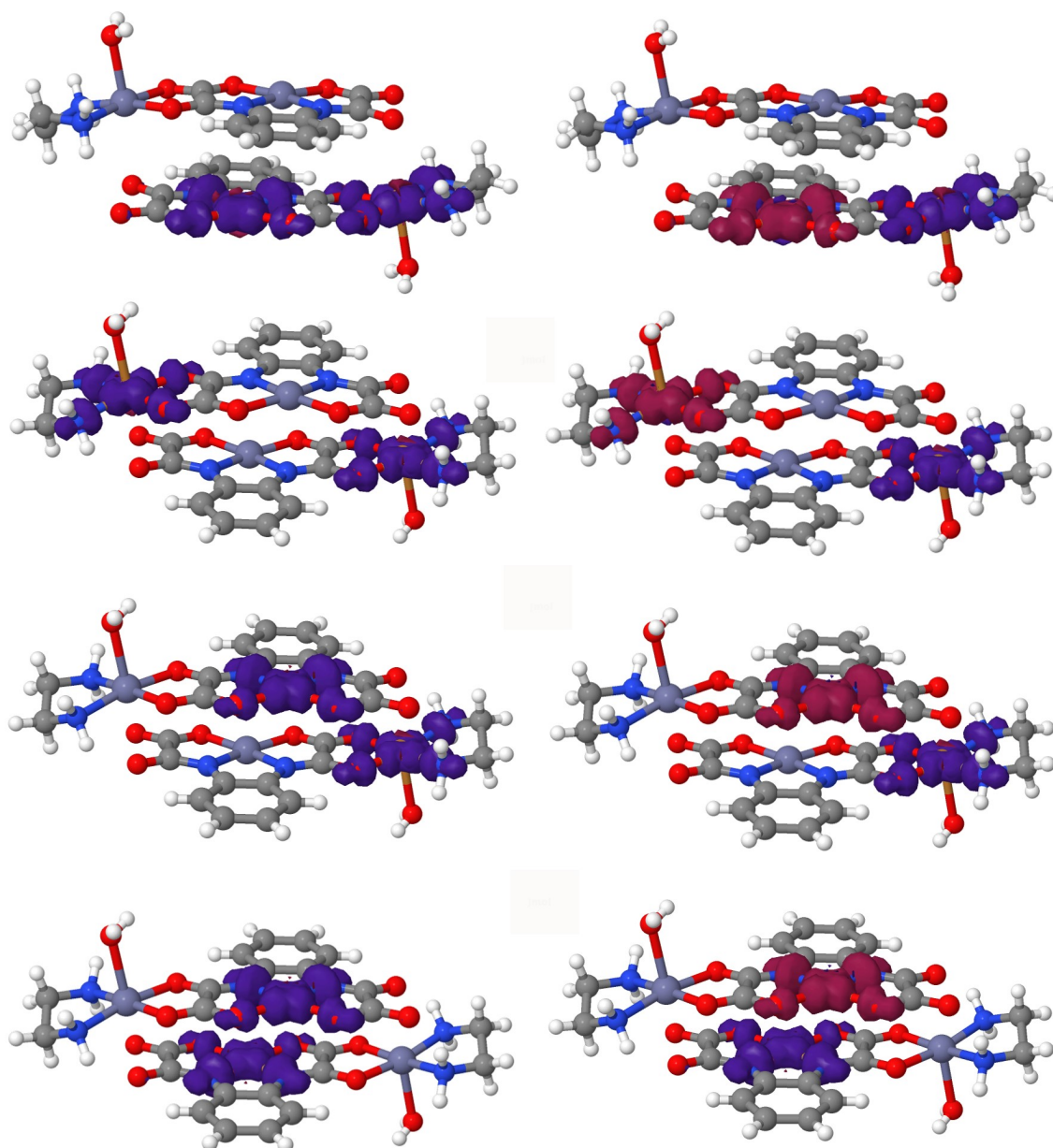


Figure S11: spin density for the triplet (high-spin, left) and its respective broken symmetry (right) states, with contour value 0.002 a.u., for compound **3** tetranuclear dimer. Each pair of states (left and right) was used for the calculation of a coupling constant in Table S9. Positive values are blue, and negative, red. Color code: Cu (yellow), N (blue), O (red), H (white), C (gray), Zn (dark gray).

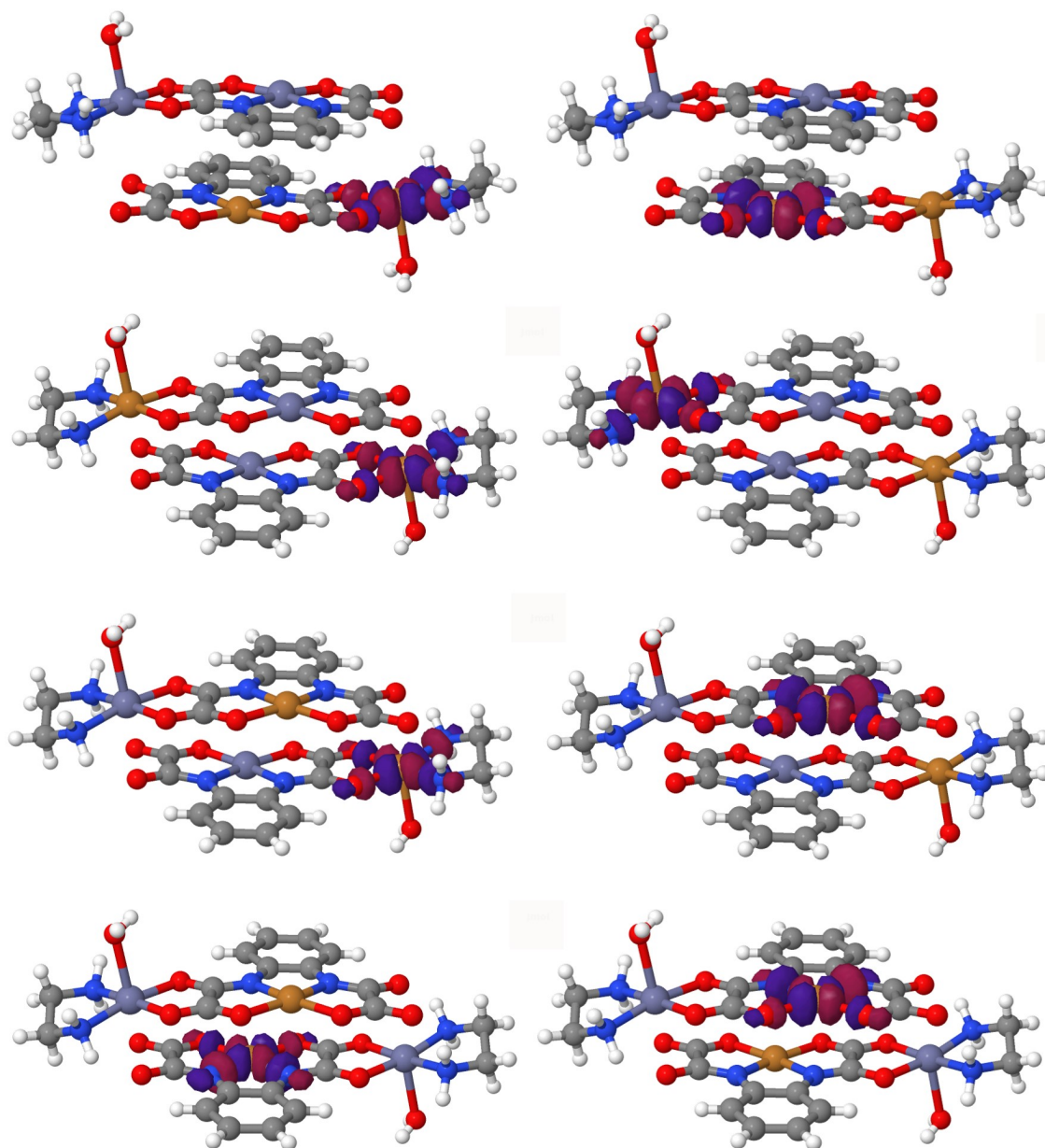


Figure S12: pair of corresponding orbitals (left and right), with contour value 0.04 a.u. for compound **3** tetranuclear dimer, for each broken symmetry state in Figure S11 (the same order, from top to bottom, was used). Positive values are blue, and negative, red. Color code: Cu (yellow), N (blue), O (red), H (white), C (gray), Zn (dark gray).

References

- 1 R. Costa, D. Reta, I. D. P. R. Moreira and F. Illas, *J. Phys. Chem. A*, 2018, **122**, 3423–3432.
- 2 R. Valero, R. Costa, I. De P. R. Moreira, D. G. Truhlar and F. Illas, *J. Chem. Phys.*, 2008, **128**, 1–8.
- 3 E. A. Buvaylo, V. N. Kokozay, V. G. Makhankova, A. K. Melnyk, M. Korabik, M. Witwicki, B. W. Skelton and O. Y. Vassilyeva, *Eur. J. Inorg. Chem.*, 2018, **2018**, 1603–1619.
- 4 G. David, F. Wennmohs, F. Neese and N. Ferré, *Inorg. Chem.*, 2018, **57**, 12769–12776.
- 5 Mayer., *Chem. Phys. Lett.*, 1984, **110**, 445–446.
- 6 P. O. Löwdin, *Adv. Quantum Chem.*, 1970, **5**, 185–199.
- 7 I. Mayer, *Theor. Chim. Acta*, 1985, **67**, 315–322.
- 8 I. Mayer, *J. Comput. Chem.*, 2006, **28**, 204–221.
- 9 E. Ruiz, A. Rodríguez-Forteza, J. Cano, S. Alvarez and P. Alemany, *J. Comput. Chem.*, 2003, **24**, 982–989.
- 10 N. V. Reis, W. P. Barros, W. X. C. Oliveira, C. L. M. Pereira, W. R. Rocha, C. B. Pinheiro, F. Lloret, M. Julve and H. O. Stumpf, *Eur. J. Inorg. Chem.*, 2018, **2018**, 477–484.
- 11 C. Adamo and V. Barone, *J. Chem. Phys.*, 1999, **110**, 6158–6170.
- 12 A. D. Becke, *J. Chem. Phys.*, 1993, **98**, 5648–5652.
- 13 C. Lee, W. Yang and R. G. Parr, *Phys. Rev. B*, 1988, **37**, 785–789.
- 14 Y. Zhao and D. G. Truhlar, *Theor. Chem. Acc.*, 2008, **120**, 215–241.
- 15 T. Yanai, D. P. Tew and N. C. Handy, *Chem. Phys. Lett.*, 2004, **393**, 51–57.
- 16 A. D. Becke, *J. Chem. Phys.*, 1993, **98**, 1372–1377.
- 17 Y. S. Lin, G. De Li, S. P. Mao and J. Da Chai, *J. Chem. Theory Comput.*, 2013, **9**, 263–272.